

## On the Uncertainties of a Structural Model

Giora Maymon<sup>1</sup>

**Abstract:** In the last decade, probabilistic analysis was incorporated into the design process of structural elements and systems, using analytical methods and computational algorithms, which were developed for this purpose. Nevertheless, in such process there is always the question of the validity of the applied model. In this presentation, a method, which enables the inclusion of a random variable or process into the model, is described. These parameters are selected so that existing experimental results can be included in the probabilistic model, thus incorporating uncertainties of the simulation model in the analysis. Two examples are described.

### 1 Introduction

The importance of probabilistic analysis in the design process of structural elements and structural systems is well recognized today. Analytical methods and computational algorithms were developed, and are used in many design establishments and in R&D institutes. Randomness in structural geometric and dimensional parameters, material properties, allowable strength and external loads can now be treated during the design process.

All these analyses are based on a model which is built for the designed structure, either by a closed form expressions or an algorithm, like a finite element computer code. A question may be asked about the validity of the model itself, which certainly has some uncertainties in it. Not always the model used in the solution of a problem truly describes the behavior of the observed system, and in many cases the discrepancy between the observed experimental results and the model presents a random behavior. A well-known example is the buckling of a simply supported beam-column. The classical buckling load predicted by using the Euler model is never met when experimental results are analyzed. We now know that this happens because of the initial imperfections of the original beam-column. Bending moments are created in the beam, and the bending stresses induce a nonlinear behavior of the structure, causing the collapse of the beam-column when the com-

---

<sup>1</sup> (Retired) RAFAEL Ltd, P.O.B. 2250 Haifa 31021, Israel.  
Email: gioram@netvision.net.il

pressive external force is lower than the Euler buckling load. These imperfections, which are generated during the manufacturing phase of the beam, may be random in their magnitudes. Results from experiments of many “identical” specimens show dispersion in the value of the buckling load. Similar phenomena are observed in experimental results of plates and shells buckling.

There is no way to avoid modeling in an intelligent design process. This is especially true for large projects in which many sub-systems comprise the final product, where time to design and manufacture a prototype is long, and when the number of tests is limited. In the aerospace industry, products are frequently manufactured in small quantities (e.g. the space telescope, a satellite for a given mission, the small number of space shuttles, the Martian Lander, a special purpose aircraft). The problem of verification of their reliability is not similar to the reliability verification of consumer goods, where a large number of tests can be conducted and statistical estimates can be verified. In some cases, complete tests are not possible at all. Therefore, in large projects of this kind, the importance of models is enhanced. Once a model is built and verified, simulations that use it can be conducted instead of real tests. The collection of product’s performance data can be replaced by these “model simulations”, including extreme points in the required performance envelope that cannot usually be tested.

Probabilistic models, which enable the determination of the probability of failure of structural elements and structural systems, lead to the reliability of the structure which can be estimated and verified through the model, and incorporated into the reliability analysis of the system as a whole. It is clear that in such cases, incorporation of model uncertainties is extremely important. When building a model, many assumptions are made. Sometimes, the influence of some parameters is intentionally neglected, with the proper justification. In many cases there are parameters whose influence cannot be evaluated due to ignorance. Suppose that nobody thought about the initial imperfection and the possibility of these influencing the buckling load of a beam-column. Then, the available model (e.g. the Euler buckling load) is unable to describe the real behavior of the structure, as observed from experiments. When there is a discrepancy between carefully controlled experiments and a model, something is wrong with the model. These discrepancies can originate from some (unknown?) parameters or physical phenomena that were not included in the model, and the designer is unaware of.

In many cases this uncertainty in the model can be formulated using an additional random variable or random process. Using this methodology, the model, which includes now a “device” which takes care of the model uncertainties, can predict probabilistic behavior of the structure that will be in agreement with the experimental result. In the following Chapters, two examples are demonstrated.

## 2 Probabilistic model for Beam-Column buckling

The proposed approach is demonstrated on the Euler buckling model discussed earlier. A beam-column of length  $L$ , width  $b$  and thickness  $h$ , made of a material with Young's modulus  $E$  is subjected to an axial compressive force  $P$ . The model is shown in Figure 1.

When the beam is perfectly straight, the buckling load is given by the Euler critical load, which is a solution of the eigenvalue equation.

$$P_{cr} = \frac{\pi^2 EI}{L^2} \quad (1)$$

where  $I$  is the cross section moment of inertia, which in this case is:

$$I = \frac{bh^3}{12} \quad (2)$$

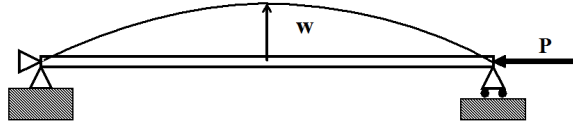


Figure 1: A Simply Supported Beam-Column Under Axial Compression

According to this solution, the column will not have any lateral deflections when the force  $P$  is increased from zero to  $P_{cr}$ , and will collapse when the force reaches the critical value  $P_{cr}$ . The lateral deflection at this point will tend to infinity. If the beam has an initial lateral deflection  $w_0$ , increase of the load creates lateral deflection  $w$ . Assuming the initial deflection is half sine wave with amplitude  $a_0$ :

$$w_0 = a_0 \sin \frac{\pi x}{L} \quad (3)$$

It can be shown that in this case, the lateral deflection  $w$  is given by

$$w = a_0 \sin \frac{\pi x}{L} \cdot \frac{\frac{P}{P_{cr}}}{1 - \frac{P}{P_{cr}}} \quad (4)$$

For any given  $x$ , Eq. (4) describes a non-linear relation between the lateral deflection  $w$  and the applied force  $P$ . Due to the lateral deflection there is a bending

moment in the beam, which has a maximum at the beam center,  $x = L/2$ . This moment creates bending stresses. In addition to these there are compression stresses due to the axial force itself. Suppose that the material fails when the total local stress reaches a value of  $\sigma_{max}$ . When  $\sigma_{max}$  is reached, the beam collapse while the acting force  $\mathbf{P}$  is smaller than the Euler critical value  $P_{cr}$ .

In reality, initial imperfections may be a combination of many sine waves along the beam, but they can be described by a Fourier series of amplitudes (that may be random) for many wave lengths. In what follows only one half sine wave is used, without a loss of generality, because expressions similar to Eq. (4) can be obtained for every combination of initial waves.

In Figure 2, the absolute maximum stress in the mid-length is described as a function of  $\mathbf{P}$  for several values of  $a_0$ . The thicker L shaped line shows the Euler solution. The numerical values used for the example are:

$$\begin{aligned} L &= 60 \text{ cm} \\ b &= 8 \text{ cm} \\ h &= 0.5 \text{ cm} \\ E &= 2100000 \text{ kgf/cm}^2 = 29842 \text{ ksi} \\ \sigma_{max} &= 5000 \text{ kgf/cm}^2 = 71 \text{ ksi} \end{aligned} \quad (5)$$

The Euler buckling force in this case is:

$$P_{cr} = 479.77 \text{ kgf} = 1056.76 \text{ Lbs.} \quad (6)$$

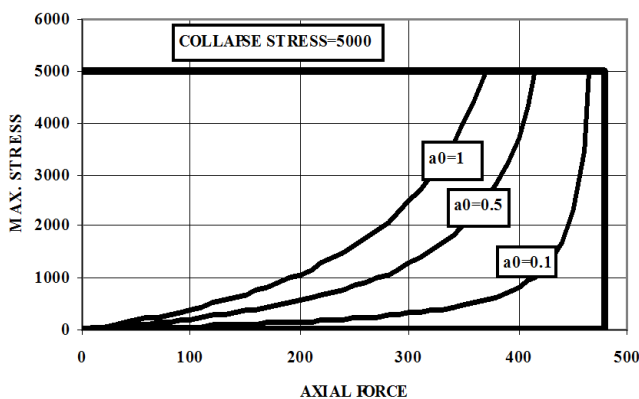


Figure 2: Stress in Mid-Beam for 3 Values of Imperfection. Euler Load=479.77 kgf

As we do not have experimental results for this case, such results will be “manufactured” artificially. It is assumed that the specimens in the “experiments” have a half sine-wave initial imperfection, with amplitude  $a_0$  which has a lognormal distribution with **mean=0.15** cm and **standard deviation=0.07** cm. The location and shape parameters for this case are  **$m=-1.9956338$**  and  **$s=0.443878028$** . The distribution of the imperfection amplitudes is shown in Figure 3.

With this distribution, “virtual experimental data” can be created for  $P_{ratio}$ - the ratio of the collapse force (the force that creates a stress of  $5000\text{kgf}/\text{cm}^2$  in the beam) to the Euler buckling force. The computations were done running 5000 Monte-Carlo simulations with MATLAB.

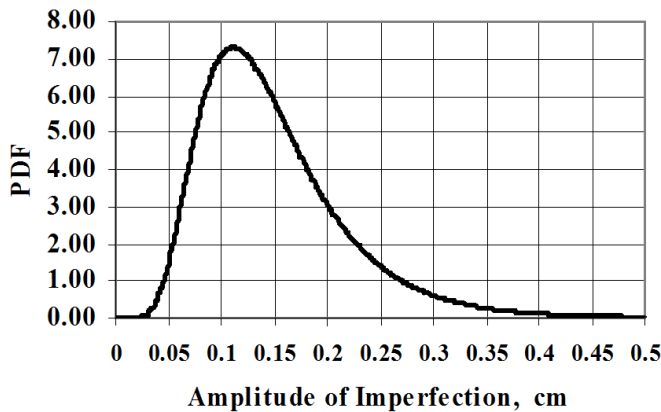


Figure 3: PDF of the Amplitude of Imperfection(Lognormal). **Mean=0.15**, **SD=0.07**

The histogram of the results is described by square symbols in Figure 4. The mean of these results is  $\mu = 0.958$  and the standard deviation is  $\sigma = 0.01803$ . A Weibull distribution with the same mean and standard deviation was fitted to this data, and is shown in full line in Figure 4. The parameters of the Weibull distribution obtained are:

$$\begin{aligned}
 \mu &= \text{mean} = 0.958 \\
 \sigma &= \text{standard deviation} = 0.01803 \\
 \alpha \text{ parameter} &= 67.42607 \\
 \beta \text{ parameter} &= 0.9660698
 \end{aligned}
 \tag{7}$$

It can be seen that the fitted distribution agrees very well with the “experimental” results.

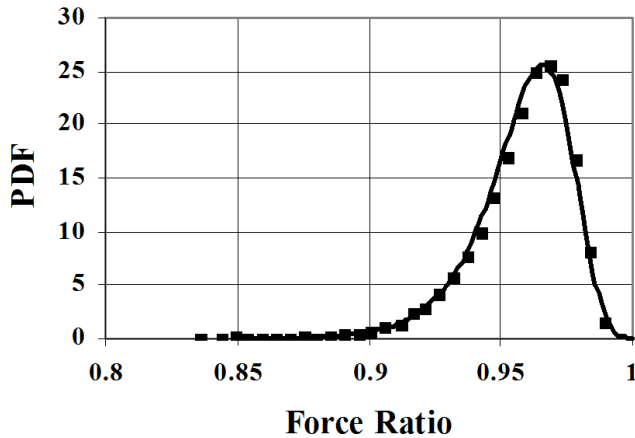


Figure 4: Distribution of “Experimental” Force Ratio (squares) and Fitted Weibull Distribution (solid line)

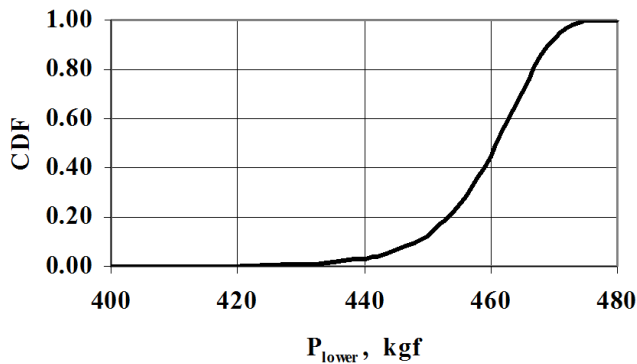


Figure 5: Probability that Collapse Load is Lower than  $P_{lower}$

A model for the collapse load based on the Euler buckling load and includes the model uncertainty can now be written as:

$$P_{collapse} = \frac{\pi^2 EI}{L^2} \cdot P_{ratio} \quad (8)$$

$P_{ratio}$  is an **added random variable** which has a Weibull distribution shown in Figure 4, with the parameters given in Eq. (7).

Assuming that E, I and L are deterministic, and the only random variable is  $P_{ratio}$  (e.g. only model uncertainty exists), one can calculate the probability that the col-

lapse load will be lower than a given value  $P_{lower}$ . Results computed using NESSUS program, are shown in Figure 5. A similar computation can be performed assuming that the geometry parameters (L, b and h) and material property (E) are also random.

### 3 Probabilistic model for crack propagation

Models for crack growth have been the subject of thousands of papers published over the past 40 years. These ranges from simplified to more advanced models, most of them are based on experimental observations. The most basic model is the one suggested by Paris and Erdogan [Paris and Erdogan (1963)], where the rate of crack growth is described by:

$$\frac{da}{dN} = C \cdot (\Delta K_I)^n \quad (9)$$

where  $a$  is the crack length,  $N$  is the number of load cycles,  $\Delta K_I$  is the stress intensity factor,  $C$  and  $n$  are material properties extracted from tests. There are models which includes the effects of the stress ratio  $R$  (i.e. Forman equation, which is used in the NASGRO computer code), with corrections for crack closure phenomena, and the “unified” approach model suggested by Vasudevan and al.(e.g. [Vasudevan, Sadananda and Galinka (2001); Sadananda and Vasudevan (2003)]). All these models are deterministic.

When tests are performed on many “identical” specimens, typical results look like those in Figure 6 (e.g. [Virkler (1979); Ghenom and Dore (1987)]).

These results are characterized by three major properties:

- (1) The behavior of crack length **is random**, even when very carefully controlled experiments are performed with “identical” specimens;
- (2) The crack length behavior is **non-linear**;
- (3) The curves of different specimens **intermingle**.

When the growth rate  $da/dN$  is plotted against the stress intensity factor, experimental results yield the experimental circles depicted in Figure 7. On a log-log scale, the straight line shown is, in fact, the Paris Law. The Forman law can model the rise toward infinity at the fracture toughness value. Thus, these are models, which describe the mean behavior of the experimental data, but not the randomness expressed by the scatter in the experimental results, and therefore there is an uncertainty in the model.

There were many attempts to formulate a stochastic crack growth law. In some of them (e.g. [Lawrence, Liu, Besterfield and Belytchko (1990)]), the material constants  $C$  and  $n$  were considered as random variables. This approach suffers from

a serious **physical interpretation** – randomizing these constants also randomize their units. Also, the use of this approach does not describe the intermingling of the curves (Figure 6) which is observed experimentally.

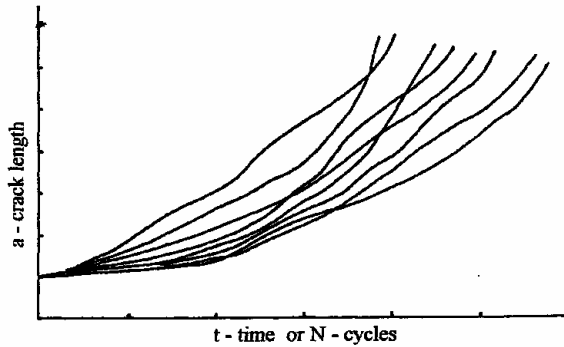


Figure 6: Generic Curves for Crack Size as a Function of Time or Cycle

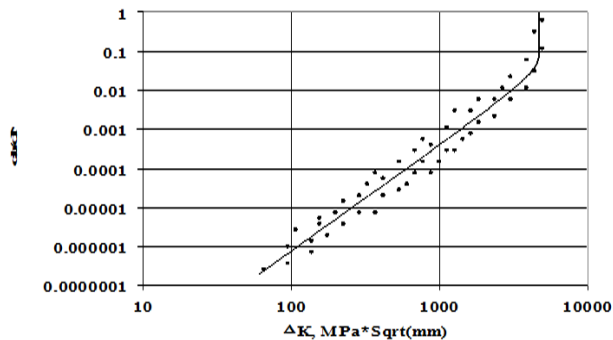


Figure 7: Crack Growth Rate vs. Stress Intensity Factor

Similar to the approach demonstrated for the Euler buckling model in the previous Chapter, it was suggested (e.g., [Lin, Wu and Yang (1984)]) to write the crack growth model in the following form:

$$\frac{da}{dN} = Q \cdot a^b \cdot X(t) \quad (10)$$

Eq. (10) can be expressed in the following logarithmic form:

$$\log\left(\frac{da}{dt}\right) = b \cdot \log(a) + \log(Q) + \log[x(t)] \quad (11)$$

or

$$Y = bU + q + z \tag{12}$$

The first two terms in Eq. (12) describe a straight line with a slope  $b$  and a vertical axis intersection  $q$ . The  $z = \log(x)$  is a normal random process with zero mean and a standard deviation  $\sigma_z$ . The constants  $b$  and  $q$  can be estimated by linear regression of plots similar to Figure 7. The linear regression also yields a value for  $\sigma_z = \sigma_{\log(x(t))}$ . Once this is known the mean and standard deviation of  $x(t)$  can then be calculated by the normal to lognormal conversion formulas (see, e.g., Eq. (13.8) in ref. [Maymon (1998)]). In ref. [Lin, Wu and Yang (1984)], the following values were obtained from experimental results of a specific case:

$$\begin{aligned} b &= 0.9297 \\ Q &= 1.1051 \cdot 10^{-4} \\ \mu_x &= 1.0206 \\ \sigma_{\log(x)} &= 0.087635 \end{aligned} \tag{13}$$

For these values, random processes  $z(a)$  with a normal distribution with  $\sigma_{\log(x)} = 0.087635$  were created using random generator computer program. Four such processes are shown in Figure 8.

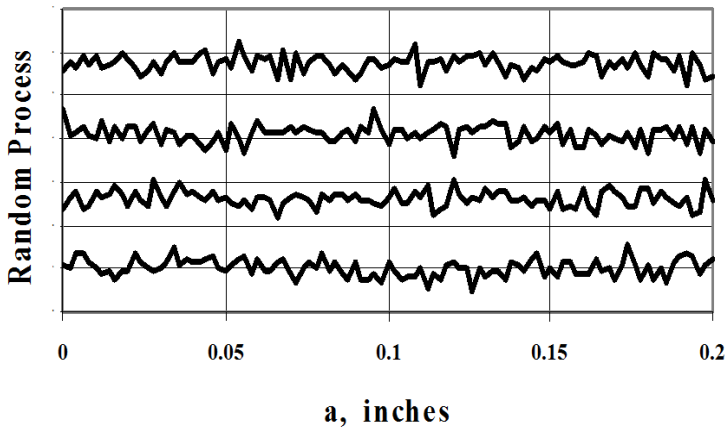


Figure 8: Four normally distributed random processes with  $\sigma_{\log(x)} = 0.087635$

In Figure 9, data points for  $da/dt$  vs.  $a$  are shown. Such results are similar to those found in experimental tests, e.g. Figure 7.

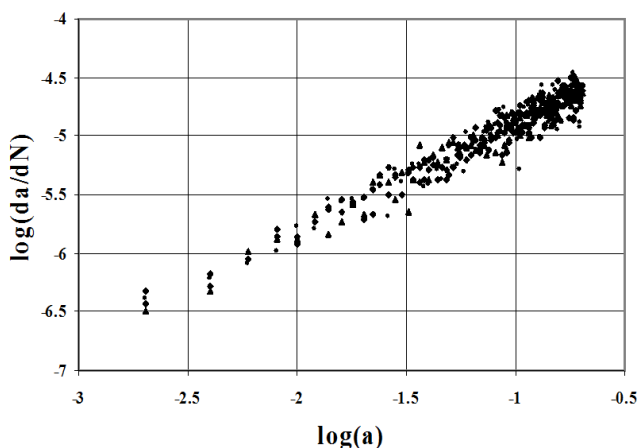


Figure 9: Scattered  $da/dn$  vs.  $a$  points, log-log scale.

As the crack growth is a local phenomenon, the stochastic process is correlated only within a certain distance near the crack tip. There are some suggestions (e.g. [Lin, Wu and Yang (1984); Sobczyk (1984); Sobczyk (1986)]) how to select this correlation time. When the stochastic approach is applied, results obtained show both the **nonlinear behavior** of the crack's length and the **intermingling** phenomena, thus better describe the experimental results.

#### 4 Summary

The parameters of either a stochastic variable or a stochastic process can be determined from experimental results of a case where uncertainties in the model are looked for. Thus, they can represent properly, in a probabilistic way, the uncertainties in the model. This can be done even when the reasons for these uncertain outcomes are not completely understood, and the effects of uncertainties are introduced in an "integral" way. More on the subject can be found in Ref. [Maymon (2008)]. In this way, uncertainties of a model can be included, based on the observed experimental results of a specific case.

#### Reference

**The NESSUS Structural Probabilistic Analysis Code.** Details in <http://www.nessus.swri.org>

**Paris, P. C.;Erdogan, F.(1963):** A Critical Analysis of Crack Propagation Laws. *Journal of Basic Engineering*, vol.85, no.1963, pp.528-534.

**NASGRO Crack Propagation Computer Program.** Details in <http://www.nasgro.swri.org>

**Vasudevan, A. K.; Sadananda, K.; Galinka, G.**(2001): Critical Parameters of Fatigue Damage. *International Journal of Fatigue*, vol.23(s1), pp.s39-s53.

**Sadananda, K.; Vasudevan, A. K.**(2003): Multiple Mechanism Controlling Fatigue Crack Growth. *Fatigue and Fracture of Engineering Materials and Structures*, vol.26, no.9, pp.835-845.

**Virkler, D. A. et al.**(1979): The Statistical Modelling Nature of a Fatigue Crack Propagation. *Journal of Engineering Materials and Technology*, vol. 10, no.4, pp.143-153.

**Ghenom, H.; Dore, S.**(1987): Experimental Study of Constant Probability Crack Growth Under Constant Amplitude Loading. *Engineering Fracture Mechanics*, vol. 27, no.1, pp.1-66.

**Lawrence, M.; Liu, W. K.; Besterfield, G.; Belytchko, T.**(1990): Fatigue Crack Growth Reliability. *Journal of Engineering Mechanics*, vol.116, no.3, pp.696-708.

**Lin, Y. K.; Wu, J. N.; Yang, J. N.**(1984): Stochastic Modeling of Fatigue Crack Propagation in Proceedings of the IUTAM Symposium On Probabilistic Methods in Mechanics of Solids and Structures, Stockholm, Sweden, pp. 103-110.

**Maymon, G.**(1998):*Some Engineering Applications in Random Vibrations and Random Structures*, AIAA Book Publishing.

**Sobczyk, K.**(1984): Stochastic Modeling of Fatigue Crack Growth in Proceeding of the IUATM Symposium On Probabilistic Methods in Mechanics of Solids and Structures, Stockholm, Sweden, pp.111-119.

**Sobczyk, K.**(1986): Modeling of Random Fatigue Crack Growth. *Engineering Fracture Mechanics*, vol. 24, no.4, pp.609-623.

**Maymon, G.**(2008): *Structural Dynamics and Probabilistic Analyses for Engineers*, Elsevier, Ma., USA.

